Inorganica Chimica Acta 512 (2020) 119893

Contents lists available at ScienceDirect

Inorganica Chimica Acta

journal homepage: www.elsevier.com/locate/ica

Research paper

Synthesis, characterization, luminescence properties of copper(I) bromide based coordination compounds

Chanchan Xu[a], Yuzhe Li[f], Le Lv[b], Fang Lin[a], Feng Lin[b], Zhijuan Zhang[d,e], Chaoyun Luo[b], Dawei Luo[a,b,*], Wei Liu[c,*]

[a] Hoffmann Institute of Advanced Materials, Shenzhen Polytechnic, 7098 Liuxian Blvd, Nanshan District, Shenzhen 518055, China
[b] School of Applied Chemistry and Biological Technology, Shenzhen Polytechnic, 7098 Liuxian Blvd, Nanshan District, Shenzhen 518055, China
[c] School of Chemical Engineering and Technology, Sun Yat-Sen University, Zhuhai 519082, China
[d] Institute of Mass Spectrometer and Atmospheric Environment, Jinan University, Guangzhou 510632, China
[e] College of Pharmacy, Henan University of Chinese Medicine, Zhengzhou, Henan 450046, China
[f] Material Science and Engineering Department, University of North Texas, USA

ARTICLE INFO

Keywords:
Copper bromide
Coordination compounds
Luminescence

ABSTRACT

Two new copper bromide based coordination compounds 0D-Cu_2Br_2(3,5-dimethyl-pyridine)$_4$ (**1**) and 1D-Cu_2Br_2(5-bromo-pyrimidine)$_2$ (**2**) have been synthesized and structurally characterized. X-ray diffraction analyses reveal that the inorganic module of both compounds is Cu_2Br_2 rhomboid dimer coordinated by the organic ligands. Compound **1** is a zero-dimensional (0D) molecular complex while compound **2** is one-dimensional (1D) extended structure. Photoluminescence measurement results show that **1** emits green photoluminescence peaked at 520 nm, with an IQY of 82.4%. Compound **2** emits red photoluminescence peaked at 630 nm, with an IQY of 2.1%. Both compounds exhibit potential as rare-earth metal free lighting phosphor alternatives.

1. Introduction

Inorganic-organic hybrid structures are composed of inorganic and organic modules blended at the atomic or molecular scale [1–3]. Such incorporation of both components into one structure at molecular level not only combines the properties of either component, but also generates new and interesting properties [4–12]. These types of materials have been reported several decades ago, however, they have attracted tremendous attention these days due to their optoelectronic applications [13–17]. One of the hybrid structural families, the copper halide based hybrids, have been found to be excellent luminescent materials that exhibit potential as efficient and rare-earth element (REE) free light-emitting phosphors, due to the fact that most of the commercial phosphors contain rare-earth metals, which have potential supply risk [18–24].

Most of the previous work on copper halide based inorganic–organic hybrid structures have been focused on copper iodide based structures [25–27]. Copper bromide and copper chloride based hybrids have been much less investigated [8,28]. Various inorganic modules have been found for copper halide based structures, including CuX monomer, Cu_2X_2 rhomboid dimer, Cu_4X_4 cubane tetramer, CuX staircase chain, etc. Based on previous studies, Cu_2X_2 rhomboid dimer based structures generally exhibiting strong photoluminescence [18,28]. The luminescence mechanism of copper halide dimer based structures is reported to be a combination of metal-to-ligand charge transfer (MLCT) and halide-to-metal charge transfer (XLCT) as reported for other copper halide dimer based structures [29–33]. It is worth mentioning that in recent years, numerous light-emitting all-inorganic copper halides have been reported, and their emissions are majorly from self-trapped excitons [34,35]. They can also be lead-free sensitive X-ray scintillators [36]. Though there are numerous reports on luminescence copper halide hybrids, compounds with high quantum efficiency are still interesting due to their potential applications as REE free lighting materials. Also red-light-emitting hybrid compounds are very rare and is worth studying since they are useful for generating warm white light [22].

Here, we report the synthesis of two new CuBr based inorganic–organic hybrid structures as new members of copper halide rhomboid dimer structural family [17,21]. Two organic ligands with different aromatic ring and substituted groups have been used, and they are 3,5-dimethyl-pyridine and 5-bromo-pyrimidine, which forms a zero-dimensional hybrid structure 0D-Cu_2Br_2(3,5-dimethyl-pyridine)$_4$ (**1**) and a one-dimensional (1D) hybrid structure 1D-Cu_2Br_2(5-bromo-

* Corresponding authors at: Hoffmann Institute of Advanced Materials, Shenzhen Polytechnic, 7098 Liuxian Blvd, Nanshan District, Shenzhen 518055, China (D. Luo).
E-mail addresses: luodw@szpt.edu.cn (D. Luo), liuwei96@mail.sysu.edu.cn (W. Liu).

https://doi.org/10.1016/j.ica.2020.119893
Received 18 May 2020; Received in revised form 7 July 2020; Accepted 11 July 2020
Available online 15 July 2020
0020-1693/

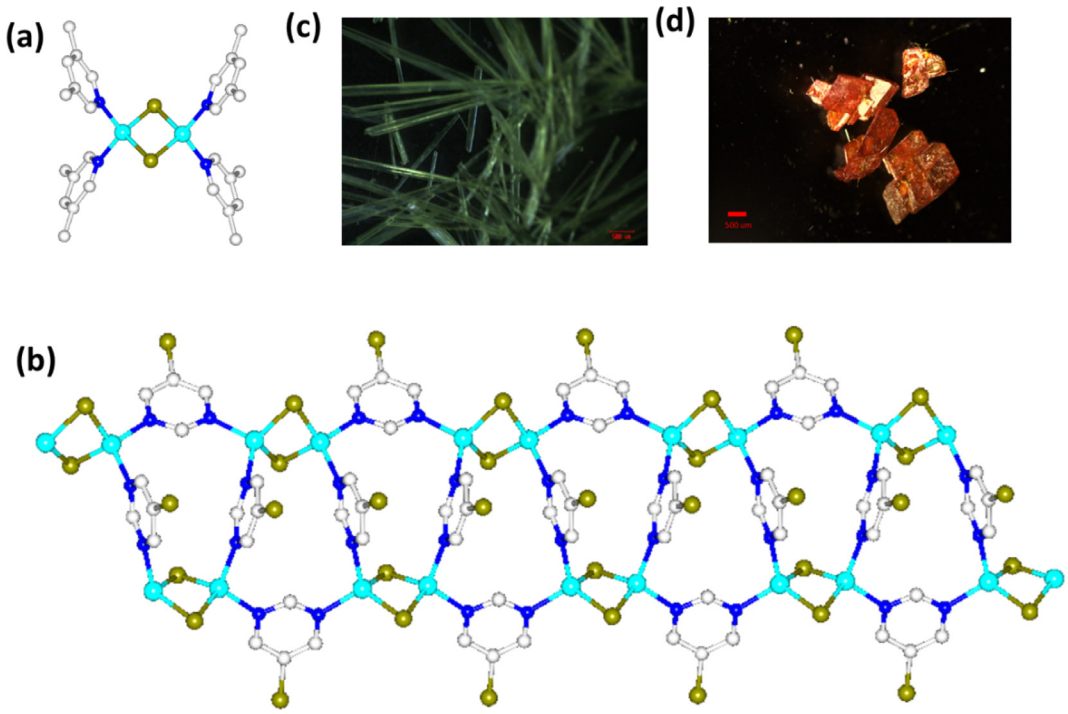

Fig. 1. (a) Structure plot of 0D-Cu_2Br_2(3,5-dimethyl-pyridine)$_4$ (**1**). (b) Structural plot of 1D-Cu_2Br_2(5-bromo-pyrimidine)$_2$ (**2**). cyan balls: Cu atoms; dark yellow: Br atoms; grey balls: C atoms.; blue balls: N atoms; hydrogen atoms were hidden for clarity. (c) Crystal image of **1**. (d) Crystal image of **2**. (For interpretation of the references to color in this figure legend, the reader is referred to the web version of this article.)

pyrimidine)$_2$ (**2**) (Fig. 1a and b). The two hybrid structures have been characterized by both single crystal and powder X-ray diffraction methods. Their thermal and optical properties have also been investigated. Compound **1** exhibits strong green photoluminescence with an internal quantum yield (IQY) as high as 82.4% under UV light excitation. Compound **2** is a red-light emitter with an IQY of 2.1%.

2. Experimental

2.1. Materials

CuBr (98%, Aladdin), KBr (> 99%, Aladdin), acetonitrile (> 99%, Aladdin), 3,5-dimethylpyridine (*3,5-dm-py*, > 98%, Aladdin), 5-bromo-pyrimidine (*5-Br-pm*, > 98%, Aladdin).

2.2. General procedure for the synthesis of (1)

Single crystals of 0D-Cu_2Br_2(*3,5-dm-py*)$_4$ (**1**) were acquired by a layering method. The reactions were conducted in glass vials. The bottom, middle and top layers were CuBr (0.015 g, 0.1 mmol)/KBr saturated aqueous solution (2 mL), acetonitrile (2 mL), and ligand (0.05 g, 0.5 mmol) in ethanol (2 mL), respectively. Rod-shaped crystals formed in the middle layer 3 days at room temperature. Pure phase powder samples were obtained by direct mixing of CuBr (0.015 g, 0.1 mmol) in saturated KBr solution (2 mL) with ligand (0.05 g, 0.5 mmol) in ethanol (2 mL). The pure phase powder generally formed immediately after stirring. The isolated yield is 64% based on Cu.

2.3. General procedure for the synthesis of (2)

1D-Cu_2Br_2(*5-Br-pm*)$_2$ was obtained under the same reaction conditions as **1**. The bottom, middle and top layers were CuBr (0.015 g, 0.1 mmol)/KBr saturated aqueous solution (2 mL), acetonitrile (2 mL), and ligand (0.05 g, 0.5 mmol) in ethanol (2 mL), respectively. Red rod-shaped crystals formed in 5 days. The isolated yield is 43% based on Cu. Pure phase powder samples were obtained by direct mixing of CuBr (0.015 g, 0.1 mmol) in saturated KBr solution (2 mL) with ligand (0.5 mmol) in ethanol (2 mL). The pure phase powder generally formed immediately after stirring.

2.4. Sample washing and drying

Upon completion of reactions, powder sample of **1** and **2** were collected by filtration from the reaction solution and washed with a small amount of acetonitrile for three times. The sample was then dried in a vacuum oven overnight before other measurements were made.

2.5. Single crystal X-ray diffraction (SXRD)

Single crystal X-ray diffraction data of **1** and **2** were collected on a Bruker-AXS smart APEX I CCD diffractometer with graphite-monochromated Mo Kα radiation (λ = 0.71073 Å). The structures were solved by direct methods and refined by full-matrix least-squares on F^2 using the Bruker SHELXTL package. The structures were deposited in the Cambridge Structural Database (CSD), and the file numbers are 1506743 and 1506744. A summary of the crystal data of the two compounds are given in Table 1.

2.6. Powder X-ray diffraction (PXRD)

PXRD analyses were carried out on a Bruker D8 Advance automated diffraction system using Cu Kα radiation (λ = 1.5406 Å). The data were collected at room temperature in a 2θ range of 3–50° with a scan speed of 1°/min. The operating power was 40 kV/40 mA.

2.7. UV–vis diffuse reflectance spectra

UV–vis diffuse reflectance spectra were measured at room temperature on a Shimadzu UV-3600 UV/VIS/NIR spectrometer. The reflectance data were converted to Kubelka–Munk function, $\alpha/S = (1 - R)^2/2R$ (α is absorption coefficient, S is scattering coefficient and R is reflectance), and used to estimate the band gap. Samples for

Table 1
Single crystal X-ray diffraction data of compound **1** and **2**.

Compound	1	2
Formula	$C_{28}H_{36}Br_2Cu_2N_4$	$C_8H_6Br_4Cu_2N_4$
Fw	715.51	604.87
Space Group	*C2/c*	*Pbcn*
a (Å)	17.823(11)	16.1765(16)
b (Å)	9.271(6)	8.3154(8)
c (Å)	20.329(13)	21.382(2)
α(°)	90.00	90.00
β(°)	114.054(10)	90.00
γ(°)	90.00	90.00
V (Å3)	3068(3)	2876.2(5)
Z	4	8
T (K)	298(2)	298(2)
λ (Å)	0.71073	0.71073
ρ ($g{\cdot}cm^{-3}$)	1.549	2.794
R_1[a] [$I > 2\sigma(I)$]	0.0423	0.0351
wR_2[a][$I > 2\sigma(I)$]	0.0868	0.0809
R_1[a] (all data)	0.0908	0.0530
wR_2[a] (all data)	0.1063	0.0886

[a] $R_1 = \Sigma||F_o| - |F_c||/\Sigma|F_o|$. $wR_2 = [\Sigma w(F_o^2 - F_c^2)^2/\Sigma w(F_o^2)^2]^{1/2}$.

reflectance measurements were prepared by evenly distributing ground powder sample between two quartz slides.

2.8. Thermogravimetric (TG) analysis

TG analyses of the title compounds were performed on a computer-controlled TG 550 (TA Instrument). Pure powder samples were loaded into platinum pans and heated with a ramp rate of 10 °C/min from room temperature to 400 °C.

2.9. DFT calculation

Band structure (BS) and density of states (DOS) calculations were performed employing density functional theory (DFT). The electronic properties of ligands were evaluated with density functional theory (DFT) computations using the Gaussian 09 suite of programs. A hybrid functional, B3LYP, was used for all calculations. Ligands were optimized using DGDZVP and 6-31 + G* basis sets, respectively [37,38].

2.10. Photoluminescence measurements

Steady-state photoluminescence spectra were obtained at room temperature on a FLS1000 spectrofluorometer.

2.11. Time-resolved photoluminescence

Time-Resolved Emission data were collected at room temperature using the FLS1000 spectrofluorometer. The dynamics of emission decay were monitored by using the FLS1000's time-correlated single-photon counting capability (1024 channels; 10 μs window) with data collection for 10,000 counts. Excitation was provided by an Edinburgh EPL-360 picosecond pulsed diode laser. The lifetime was obtained by mono-exponential fitting.

2.12. Internal quantum yield measurements

Internal quantum yield (IQY) of samples in powder form was measured on a C9920-03 absolute quantum yield measurement system (Hamamatsu Photonics) with a 150 W xenon monochromatic light source and 3.3 in. integrating sphere.

3. Results and discussion

Compound **1** and **2** have been prepared by direct mixing of the organic ligands with CuBr/KBr saturated solution at room temperature. *Cm*-sized rod-shaped single crystals are obtained (Fig. 1c and d). The ligand has been added in excess to avoid the formation of staircase chain based hybrid structure. Single crystal X-ray diffraction analysis reveals that **1** crystallizes in the monoclinic space group *C2/c*. The inorganic module of **1** is Cu_2Br_2 rhomboid dimer. The copper ions coordinate to two bromide ions and two ligand molecules in a tetrahedral geometry (Fig. 1). Single crystal X-ray diffraction analysis reveals that compound **2** crystallizes in the orthorhombic space group *Pbcn*. The inorganic module in compound **2** is also Cu_2Br_2 rhomboid dimer. Each dimer motif has been connected by the bidentate *5-Br-pm* ligands, forming a 1D extended chain. Detailed crystallographic data are summarized in Table S1. The structures of the two compounds are plotted in Fig. 1a and b. PXRD analyses have been carried out to confirm the phase purity of compound **1** and **2** (Figures S1 and S2). The peak positions of observed PXRD patterns are in good agreement with those simulated from single crystal X-ray data, indicating that pure phases are obtained. The compositions of the sample prepared were further confirmed by elemental analysis (Table S1). Details of the synthesis and characterization can be found in the Supporting Information.

The decomposition temperature of this compound **1** was estimated to be 50 °C while the decomposition temperature of this compound **2** was estimated to be 110 °C (Figures S3 and S4). The higher decomposition temperature for compound **2** is the result of the formation of extended structures.

The optical absorption spectra of compounds **1** and **2** were investigated at room temperature and are plotted in Fig. 2a. Both

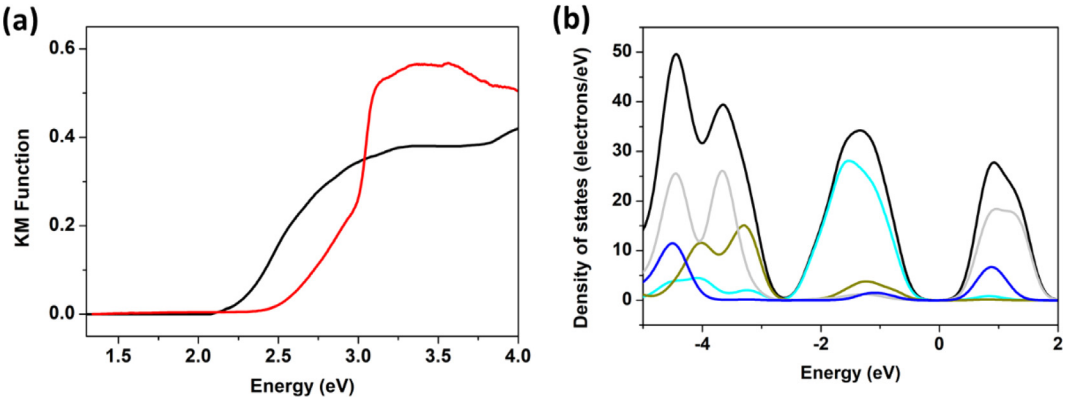

Fig. 2. (a) UV–vis absorption spectra of **1** (red) and **2** (black). (b) Calculated density of states (DOS) of **1** by DFT method: total DOS (black); Cu 3d orbitals (cyan); Br 4p orbitals (dark yellow); C 2p orbitals (grey); N 2p orbitals (blue). (For interpretation of the references to color in this figure legend, the reader is referred to the web version of this article.)

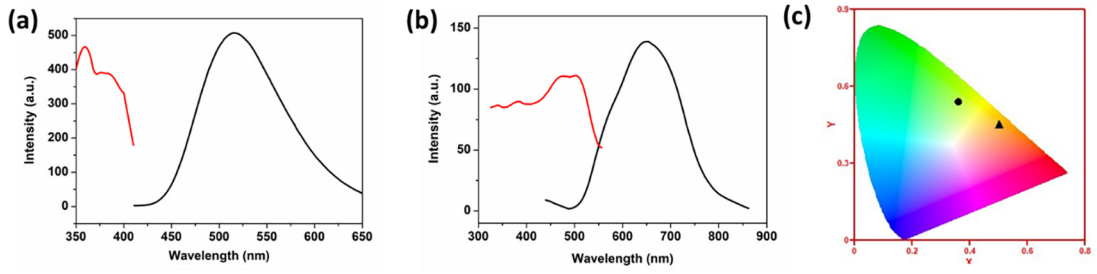

Fig. 3. (a) Excitation (red) and emission spectra (black) of **1**. (b) Excitation (red) and emission spectra (black) of **2**. λ_{ex} = 360 nm, λ_{1em} = 520 nm, λ_{2em} = 630 nm. (c) CIE coordinates of **1** (circle) and **2** (triangle). (For interpretation of the references to color in this figure legend, the reader is referred to the web version of this article.)

compounds appear to be semiconductors with direct band gap. The estimated energy gaps between the filled and empty orbitals of compounds **1** and **2** are ~2.5 and ~2.1 eV, respectively.

First-principle calculations of the band structure (BS) and density of states (DOS) of compound **1** were carried out using the CASTEP code implemented in the Material studio 5.0 package. Generalized gradient approximations (GGA) with Perdew–Burke–Ernzerhof (PBE) exchange–correlation functional (xc) were used in all calculations. The calculated band gap for compound **1** is 1.536 eV (Figure S5). DOS analysis results reveal that in both compounds, the energy states in the valence band maximum region are majorly from the inorganic components (Cu 3d and Br 4p atomic orbitals), while in the region of conduction band minimum, the major contributions are from the organic components (C and N 2p atomic orbitals) (Fig. 2b). The band gaps of **1** and **2** may be tuned by altering the halides or the organic ligands.

The organic ligands and pure CuBr emit no noticeable emission under UV excitation. Single crystals of **1** emit strong bright green light while compound **2** emits weak red light under UV irradiation (360 nm). The room temperature emission and excitation spectra are shown in Fig. 3a and 3b. The green emission peaked at 520 nm of compound **1** at room temperature has a full width at half-maximum (FWHM) of around 100 nm. The red mission peaked at 630 nm of compound **2** has a FWHM of around 110 nm. The Commission Internationale de l'Eclairage (CIE) chromaticity coordinates for compound **1** and **2** is calculated to be (0.36, 0.54) and (0.50, 0.45), respectively (Fig. 3c).

The ligands have play an important role in the band gaps and luminescence energies of the hybrid structures. We have calculated the lowest unoccupied molecular orbital (LUMO) energies of the organic ligands, and found out that the ligand with lower LUMO energy lead to the formation of hybrid structures of lower band gap and emission energy. Such phenomenon has been found for copper iodide based hybrid structures [25].

The room temperature IQYs were measured on a C9920-03 absolute quantum yield measurement system (Hamamatsu Photonics), and the values are given in Table 2. The IQYs of compound **1** and **2** are 82.4% and 2.1%, respectively, at excitation energy of 360 nm. The big IQY difference of compound **1** and **2** suggests that the structures of the organic ligands play an important role in the luminescence efficiency of this type of structures. Typically, organic ligands with electron donating groups, such as methyl group, would enhance the IQYs of the hybrid structures. While organic ligands with electron withdrawing groups, such as halide, would quench the emission of the hybrid structures.

Based on previous studies, this type of hybrid compounds with higher band gaps exhibit higher IQYs than those with lower band gaps, which is also in accordance with the energy gap law [39]. Following the same trend, Compound **1** have higher band gap and IQY compared to that of compound **2**. Based on the equation below:

$$\Phi = k_r \tau$$

Φ is quantum yield, τ is lifetime, k_r is radiative rate constant [40]. The quantum yield is directly proportional to the lifetime. Luminescence decay measurements were carried out and their τ values are 5.9 and 3.1 μs for **1** and **2**, respectively, in trend with their deceasing band gap values as well as their quantum yield values (Figure S6).

Under the photo excitation at the excited energy, the electrons are excited from the valance bands to the conduction bands, and the radiative recombination of electron and hole result in the luminescence of the compounds. The DOS pattern indicates the metal-to-ligand charge transfer (MLCT) luminescence mechanism. Both the band gaps and emission energies of this type of hybrid metal halides could be systematically tuned by selecting different organic ligands. The halides would also influence their optical properties. Their iodide analogues 0D-Cu_2I_2(3,5-dimethyl-pyridine)$_4$ and 1D-Cu_2I_2(5-bromo-pyrimidine)$_2$ have been reported and a comparison between their optical properties have been conducted [17]. The band gaps and emission maximum of 0D-Cu_2I_2(3,5-dimethyl-pyridine)$_4$ are 2.8 eV and 479 nm. Both the band gaps and emission ranges of the bromide compounds show a red-shift compared to those of the iodide analogues.

Compound **1** shows good photostability. Shining the sample of **1** with UV light for 7 days would not change the structure of the sample as confirmed by the PXRD analyses (Figure S1). Most of previously reported copper bromide based compounds show relatively lower IQY compared to copper iodide based compounds [28]. Such a high IQY for **1** indicates the potential of copper bromide based hybrid structures as light-emitting materials.

4. Conclusions

In summary, we have synthesized and characterized two copper bromide rhomboid dimer based inorganic–organic hybrid structures **1** and **2**. Compound **1** is a strong green light emitter, with an IQY of 82.4%. Compound **2** is a weak red light emitter, with an IQY of 2.1%. Both compounds show potential as rare-earth free lighting phosphor alternatives.

Declaration of Competing Interest

The authors declare that they have no known competing financial

Table 2
Summary of Photophysical Properties of **1** and **2**.

#	Band gap (eV)	λ_{ex} (nm)	Emission color	λ_{em} (nm)	IQY (%)	Lifetime (μs)	CIE	LUMO (eV)
1	2.5	360	Green	520	82.4 (± 0.4)	5.9	(0.36, 0.54)	−1.04
2	2.1	360	Red	630	2.1 (± 0.3)	3.1	(0.50, 0.45)	−1.97

interests or personal relationships that could have appeared to influence the work reported in this paper.

Acknowledgements

Financial support from the National Natural Science Foundation of China (grant no. 21901167), Shenzhen Science and Technology Innovation Commission (grant no. JCYJ20180307102051326), the Shenzhen Polytechnic Science Foundation (grant no. 6019310003K), the Post-doctoral Foundation Project of Shenzhen Polytechnic (grant no. 6019330004K) and the Pearl River Nova Program of Guangzhou (grant no. 201710010053) is gratefully acknowledged.

Appendix A. Supplementary data

Supplementary data to this article can be found online at https://doi.org/10.1016/j.ica.2020.119893.

References

[1] C.R. Kagan, D.B. Mitzi, C.D. Dimitrakopoulos, Science 286 (1999) 945–947.
[2] D.B. Mitzi, in: Progress in Inorganic Chemistry, John Wiley & Sons, Inc., 2007, pp. 1–121, doi: 10.1002/9780470166499.ch1.
[3] B. Saparov, D.B. Mitzi, Chem. Rev. 116 (2016) 4558–4596.
[4] J. Li, R. Zhang, in: Progress in Inorganic Chemistry, John Wiley & Sons, Inc., 2011, pp. 445–504, doi: 10.1002/9781118148235.ch8.
[5] X. Huang, J. Li, J. Am. Chem. Soc. 129 (2007) 3157–3162.
[6] X. Huang, J. Li, H. Fu, J. Am. Chem. Soc. 122 (2000) 8789–8790.
[7] X. Huang, J. Li, Y. Zhang, A. Mascarenhas, J. Am. Chem. Soc. 125 (2003) 7049–7055.
[8] V.W.-W. Yam, V.K.-M. Au, S.Y.-L. Leung, Chem. Rev. 115 (2015) 7589–7728.
[9] J. Li, X.Y. Huang, in: Oxford Handbook of Nanoscience and Technology, Oxford University Press, USA, 2010, vol. 2.
[10] I. Neogi, A. Bruno, D. Bahulayan, T.W. Goh, B. Ghosh, R. Ganguly, D. Cortecchia, T.C. Sum, C. Soci, N. Mathews, S.G. Mhaisalkar, ChemSusChem 10 (2017) 3765–3772.
[11] Z. Shi, J. Guo, Y. Chen, Q. Li, Y. Pan, H. Zhang, Y. Xia, W. Huang, Adv. Mater. 29 (2017) 1605005.
[12] C. Zhou, H. Lin, H. Shi, Y. Tian, C. Pak, M. Shatruk, Y. Zhou, P. Djurovich, M.-H. Du, B. Ma, Angew. Chem. 130 (2018) 1033–1036.
[13] L. Mao, P. Guo, M. Kepenekian, I. Hadar, C. Katan, J. Even, R.D. Schaller, C.C. Stoumpos, M.G. Kanatzidis, J. Am. Chem. Soc. 140 (2018) 13078–13088.
[14] M. Yu, L. Chen, F. Jiang, K. Zhou, C. Liu, C. Sun, X. Li, Y. Yang, M. Hong, Chem. Mater. 29 (2017) 8093–8099.
[15] L. Mao, Y. Wu, C.C. Stoumpos, M.R. Wasielewski, M.G. Kanatzidis, J. Am. Chem. Soc. 139 (2017) 5210–5215.
[16] L.N. Quan, F.P. García de Arquer, R.P. Sabatini, E.H. Sargent, Adv. Mater. 30 (2018) 1801996.
[17] W. Liu, Y. Fang, G.Z. Wei, S.J. Teat, K. Xiong, Z. Hu, W.P. Lustig, J. Li, J. Am. Chem. Soc. 137 (2015) 9400–9408.
[18] W. Liu, Y. Fang, J. Li, Adv. Funct. Mater. 28 (2018) 1705593.
[19] W. Liu, K. Zhu, S.J. Teat, G. Dey, Z. Shen, L. Wang, D.M. O'Carroll, J. Li, J. Am. Chem. Soc. 139 (2017) 9281–9290.
[20] R. Peng, M. Li, D. Li, Coord. Chem. Rev. 254 (2010) 1–18.
[21] K. Tsuge, Y. Chishina, H. Hashiguchi, Y. Sasaki, M. Kato, S. Ishizaka, N. Kitamura, Coord. Chem. Rev. Part 2 (2016, 306,) 636–651.
[22] X. Huang, Nat. Photonics 8 (2014) 748.
[23] P.M. Pattison, J.Y. Tsao, G.C. Brainard, B. Bugbee, Nature 563 (2018) 493–500.
[24] H. Zhu, C.C. Lin, W. Luo, S. Shu, Z. Liu, Y. Liu, J. Kong, E. Ma, Y. Cao, R.-S. Liu, X. Chen, Nat. Commun. 5 (2014) 4312.
[25] X. Zhang, W. Liu, G.Z. Wei, D. Banerjee, Z. Hu, J. Li, J. Am. Chem. Soc. 136 (2014) 14230–14236.
[26] J.-H. Jia, X.-L. Chen, J.-Z. Liao, D. Liang, M.-X. Yang, R. Yu, C.-Z. Lu, Dalton Trans. 48 (2019) 1418–1426.
[27] S.-L. Li, F.-Q. Zhang, X.-M. Zhang, Chem. Commun. 51 (2015) 8062–8065.
[28] W. Liu, W.P. Lustig, J. Li, EnergyChem 1 (2019) 100008.
[29] Q. Benito, X.F. Le Goff, S. Maron, A. Fargues, A. Garcia, C. Martineau, F. Taulelle, S. Kahlal, T. Gacoin, J.-P. Boilot, S. Perruchas, J. Am. Chem. Soc. 136 (2014) 11311–11320.
[30] S. Perruchas, X.F. Le Goff, S. Maron, I. Maurin, F. Guillen, A. Garcia, T. Gacoin, J.-P. Boilot, J. Am. Chem. Soc. 132 (2010) 10967–10969.
[31] P.C. Ford, E. Cariati, J. Bourassa, Chem. Rev. 99 (1999) 3625–3648.
[32] K.R. Kyle, C.K. Ryu, P.C. Ford, J.A. DiBenedetto, J. Am. Chem. Soc. 113 (1991) 2954–2965.
[33] F. Sabin, C.K. Ryu, P.C. Ford, A. Vogler, Inorg. Chem. 31 (1992) 1941–1945.
[34] R. Roccanova, A. Yangui, G. Seo, T.D. Creason, Y. Wu, D.Y. Kim, M.-H. Du, B. Saparov, ACS Mater. Lett. 1 (2019) 459–465.
[35] R. Roccanova, A. Yangui, H. Nhalil, H. Shi, M.-H. Du, B. Saparov, ACS Appl. Electronic Mater. 1 (2019) 269–274.
[36] B. Yang, L. Yin, G. Niu, J.-H. Yuan, K.-H. Xue, Z. Tan, X.-S. Miao, M. Niu, X. Du, H. Song, E. Lifshitz, J. Tang, Adv. Mater. 31 (2019) 1904711.
[37] N. Godbout, D.R. Salahub, J. Andzelm, E. Wimmer, Can. J. Chem. 70 (1992) 560–571.
[38] C. Sosa, J. Andzelm, B.C. Elkin, E. Wimmer, K.D. Dobbs, D.A. Dixon, J. Phys. Chem. 96 (1992) 6630–6636.
[39] R. Englman, J. Jortner, Mol. Phys. 18 (1970) 145–164.
[40] Q. Wang, Y.-J. Gao, T.-T. Zhang, J. Han, G. Cui, RSC Adv. 9 (2019) 20786–20795.